https://doi.org/10.5607/en22015
Exp Neurobiol. 2022 Jun;31(3):131-146.
pISSN 1226-2560 • eISSN 2093-8144

Review Article

Experimental Neurobiology

Cranial and Spinal Window Preparation for *in vivo* Optical Neuroimaging in Rodents and Related Experimental Techniques

Chanmi Yeon[1], Jeong Myo Im[1], Minsung Kim[1], Young Ro Kim[2,3] and Euiheon Chung[1,4,5*]

[1]Department of Biomedical Science and Engineering, Gwangju Institute of Science and Technology, Gwangju 61005, Korea, [2]Athinoula A. Martinos Center for Biomedical Imaging, Massachusetts General Hospital, Charlestown, MA 02129, [3]Department of Radiology, Harvard Medical School, Boston, MA 02115, USA, [4]AI Graduate School, Gwangju Institute of Science and Technology, Gwangju 61005, [5]Research Center for Photon Science Technology, Gwangju Institute of Science and Technology, Gwangju 61005, Korea

Optical neuroimaging provides an effective neuroscience tool for multi-scale investigation of the neural structures and functions, ranging from molecular, cellular activities to the inter-regional connectivity assessment. Amongst experimental preparations, the implementation of an artificial window to the central nervous system (CNS) is primarily required for optical visualization of the CNS and associated brain activities through the opaque skin and bone. Either thinning down or removing portions of the skull or spine is necessary for unobstructed long-term *in vivo* observations, for which types of the cranial and spinal window and applied materials vary depending on the study objectives. As diversely useful, a window can be designed to accommodate other experimental methods such as electrophysiology or optogenetics. Moreover, auxiliary apparatuses would allow the recording in synchrony with behavior of large-scale brain connectivity signals across the CNS, such as olfactory bulb, cerebral cortex, cerebellum, and spinal cord. Such advancements in the cranial and spinal window have resulted in a paradigm shift in neuroscience, enabling *in vivo* investigation of the brain function and dysfunction at the microscopic, cellular level. This Review addresses the types and classifications of windows used in optical neuroimaging while describing how to perform *in vivo* studies using rodent models in combination with other experimental modalities during behavioral tests. The cranial and spinal window has enabled longitudinal examination of evolving neural mechanisms via *in situ* visualization of the brain. We expect transformable and multi-functional cranial and spinal windows to become commonplace in neuroscience laboratories, further facilitating advances in optical neuroimaging systems.

Key words: Neuroimaging, Functional neuroimaging, Optical imaging, Central nervous system, Craniotomy, Laboratory animal models

INTRODUCTION

Recent advances in optical imaging have provided a highly effective multi-scale imaging tool for documenting various brain activities. In addition to the well-known advantages including capability for capturing microscopic images at the cellular or subcellular level, a forte of continuous monitoring of biological events with a high spatiotemporal resolution, particularly neurobiological cascades garnered high popularity among researchers of the related fields. As the image contrast, resolution, and specificity further improved with bioengineering techniques such as fluorescent proteins [1-4] and optogenetic tools [5], light-based imaging approaches are becoming increasingly higher in demand as methods for understanding neurodynamics. Additionally, the multifaceted diversity of visualization techniques such as longitudinal time-lapse imaging of the synaptic structure and function and cell-type specific imaging has also promoted the neuroscience aspect of optical imaging applications with their non-invasive nature and ease of integration with other techniques [6, 7].

In order to accomplish optical recordings of the neural, particu-

Submitted April 21, 2022, Revised June 3, 2022,
Accepted June 15, 2022

*To whom correspondence should be addressed.
TEL: 82-62-715-2753, FAX: 82-62-715-5309
e-mail: ogong50@gist.ac.kr

larly central nervous system (CNS), experimental innovation is an a priori necessity to enable the visualization of neural activities through the layers of surrounding structures. In general, the brain and spinal cord are covered with three meninges: dura mater, arachnoid mater, and pia mater while the skull and spine reside beneath the outer layer-scalp, skin, and connective tissue [8-11]. Due to their intrinsic opacity, these multiple protective layers render difficulties in the optical observation of the CNS in its natural form [12-14]. Thus, an artificial window preparation technique was developed, in which the skull is thinned down, or removed and secured with a glass coverslip [15-17]. Upon introduction, initial preparation of the cranial window (CW) was performed in large animals such as cats, rabbits, and monkeys [16, 18-20]. However, recent emergence of ethical issues and advances in optical technique have led smaller animals (e.g., rodents) as more appropriate experimental subjects. Furthering the technical improvements, the latest research shows the establishment of a spinal cord chamber window (SCCW), a surgical preparation technique modified from the dorsal skinfold chamber to observe the spinal cord optically [21-23]. In this Review, the term "central nervous system (CNS) window" will be used to refer to both the cranial window (CW) and the spinal cord chamber window (SCCW). Recently, there is a considerable demand for integrating the optical neuroimaging system with other recording modalities in conjunction with simultaneous behavioral assessments. In this regard, this Review addresses various types of the cranial and spinal windows used in rodent model studies and associated behavior tests in combination with experimental setups of multiple optical neuroimaging techniques and other recording modalities.

Compared with recent reviews related to the cranial window [24, 25], this Review introduces various structural and functional *in vivo* imaging technologies utilizing the cranial and spinal window and the various types of cranial and spinal windows in rodent models by categorizing them into ROIs, surgical preparation approaches, and window material with extensive Tables. In addition, we describe practical considerations when using the cranial and spinal window with rodent models in conjunction with other neuroscience methodologies or behavior tests with various examples.

OPTICAL NEUROIMAGING TECHNOLOGIES

Optical imaging approaches have been used to investigate structural and functional brain connections in rodents. For example, the optical neuroimaging methods such as two- or multi-photon excitation (2PE or MPE) imaging [26-29], calcium-sensitive dye imaging (calcium imaging, CaSDI) [30, 31], voltage-sensitive dye imaging (VSDI) [32-34], laser speckle contrast imaging (LSCI) [35-38], optical intrinsic signal imaging (OISI) [35, 39-42], and ultrasound imaging (USI) combined with light [43, 44] have been widely used. These techniques enabled the investigation of vascular and cellular structures, neuronal activation, blood flow, blood pressure, and oxygen saturation. In the following section, we introduce the characteristics of neuroimaging technologies.

2PE imaging became popular in neuroscience as a nonlinear laser-scanning fluorescence microscopy technique for deep-tissue cellular imaging of 500 μm~1 mm in depth and sub-micrometer spatial resolution. The two-photon excitation wavelength lies in the near-infrared range, nearly twice longer than the usual wavelengths for confocal or epifluorescence excitation. 2PE has been utilized for structural fluorescence imaging or CaSDI and VSDI for neuronal activity in wide FOV [45-48]. Recent advancement in MPE, such as 3PE, allows even deeper functional imaging beneath 1 mm depth [49].

OISI has been used to infer neural activity based on cortical reflectance change originating from hemodynamic response. OISI is used for label-free imaging of cortical functional architecture and local microcirculation with ~100 μm spatial and 1~2 sec temporal resolutions. In previous research, OISI was applied to analyze the functional connectivity in large-area of the brain cortex and even onto the mouse's exposed skull [50-52]. The oxy-/deoxy-hemoglobin concentration for specific brain regions can be estimated with multi-color light illumination [53-55].

A laser speckle is a random interference pattern from the scattering of coherent light within tissue. The fluctuations of speckle pattern caused by dynamic movements of scatters (i.e., red blood cells) within the living tissue enable a two-dimensional blood flow or tissue perfusion, called LSCI. LSCI provides a simple and powerful tool for full-field semi-quantitative functional blood flow. The spatial resolution (10 μm) and temporal resolution (10 msec to 10 sec) of LSCI can be customized depending on the specific application. Because of the limited light penetration depth, LSCI only provides superficial blood flow mapping [56, 57].

CaSDI and VSDI utilize special dyes sensitive to neuronal activity among optical neuronal imaging techniques. These approaches use dyes that generate fluorescence in response to an action potential to monitor neuronal activity in cellular or sub-cellular measurements. CaSDI and VSDI provide spatial and temporal resolutions of the μm and msec ranges, respectively. Using these methods, it is possible to simultaneously measure the neuronal activity of multiple populations within a field-of-view (FOV) [58, 59].

From the traditional optical imaging method with superficial images limited to the cortical area of an animal under anesthesia, we are witnessing deep-tissue imaging into the CNS below the cortex

https://doi.org/10.5607/en22015

of awake animals performing behavioral tasks. This advancement has been feasible with diverse cranial and spinal window models, which follow below.

DIVERSE CRANIAL AND SPINAL WINDOW MODELS

Region of interest (ROI)-based classification

The type of cranial and spinal window can be decided based on the region of interest (ROI) to be examined with the microscope. Here we describe various types of cranial windows such as the olfactory bulb [18, 60-64], somatosensory cortex [34, 35, 65, 66], visual cortex [31, 44, 67], hippocampus [68-70], cerebellum [71, 72], medial entorhinal cortex [73], and the spinal cord chamber window (SCCW) [21-23]. Fig. 1 shows the schematic diagrams of cranial and spinal windows of four representative ROIs: olfactory bulb, cerebral cortex, cerebellar cortex, and spinal cord.

Olfactory bulb window

The olfactory bulb (OB) in mammals is the initial station of the olfactory nerve pathway in the CNS [74]. The olfactory system is the only sensory organ that carries peripheral information directly to the cortex bypassing the thalamus [75]. As a result, the OB shows the combined function of the peripheral nervous system (PNS) and the thalamus within the CNS [76]. Both thinned-skull or open-skull windows can be implanted for OB imaging for studies on olfactory information processing. However, OB window preparation is challenging due to the limited frontal bone size (2.0×3.5 mm) and the location is between the eyes (Fig. 1a). Although the thinned-skull OB window enables long-term imaging, the imaging depth is further restricted due to the remaining bone and surface irregularity. In contrast, the open-skull OB window's small size necessitates repeated surgery owing to bone regrowth limiting its use only for short-term imaging. Thus, a large (~3 mm) open-skull window is suitable for long-term longitudinal imaging [62].

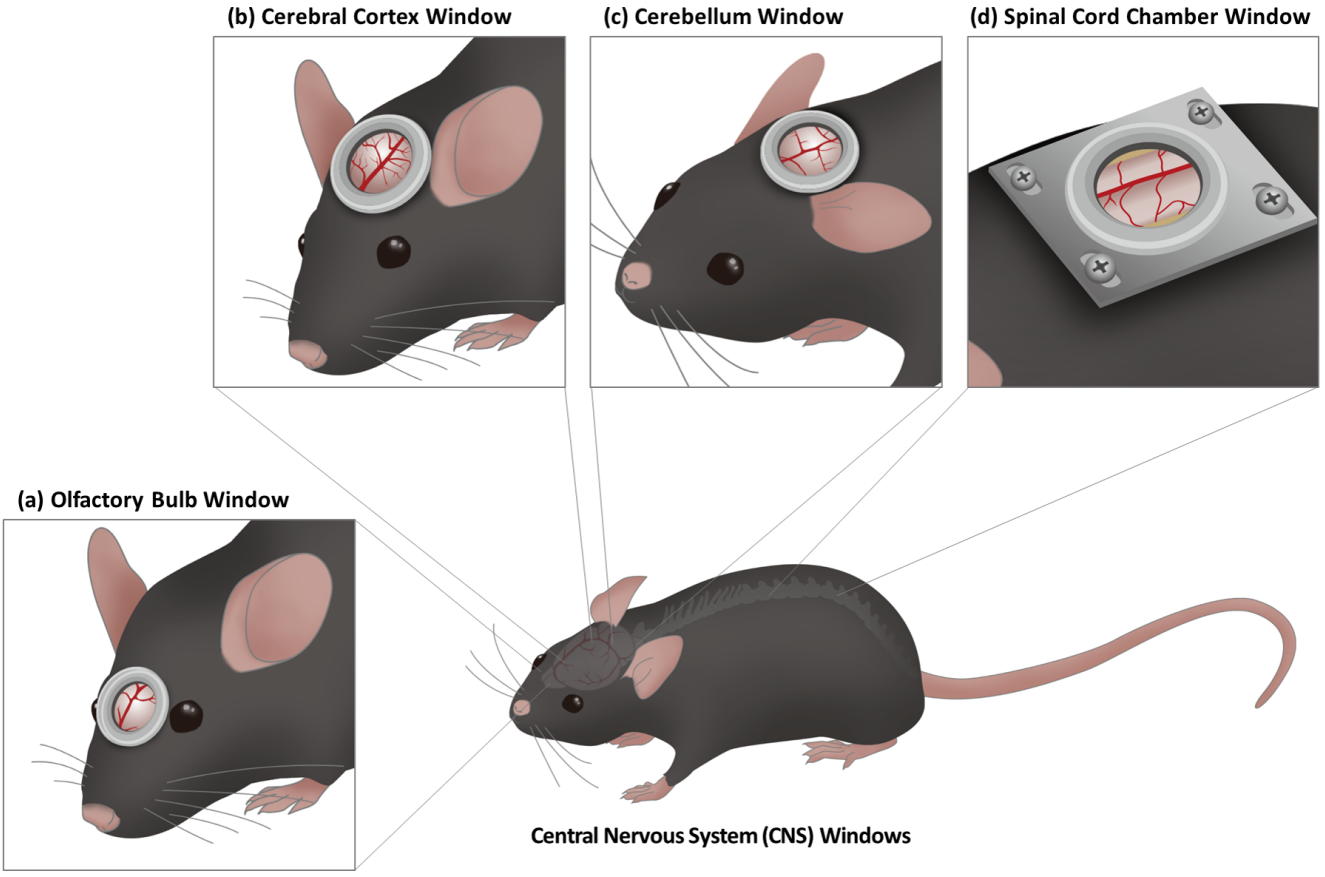

Fig. 1. Region of interest (ROI)-based cranial and spinal window classification; (a) olfactory bulb window, (b) cerebral cortex window, (c) cerebellar window, and (d) spinal cord chamber window (SCCW). The CNS consists of the brain and the spinal cord. The cranial and spinal window is advantageous for observing the outer surface of the brain and the spinal cord. The cerebral cortex is the largest and the most accessible part of the cerebrum, where the motor and the sensory areas are located. The cranial and spinal window enables observing brain connectivity during a behavioral test in brain disease models combining neuroscience methods. The cranial and spinal window and behavioral apparatus are verified.

Cerebral cortex window

The cerebral cortex is the outermost layer of the cerebrum. The entire dorsal cerebral cortex including motor and sensory areas is optically accessible after removing outer skull and scalp with transcranial window technique. The somatosensory area and barrel cortex have been common targets for studying sensory-evoked optical responses [35, 41, 65, 77]. In stroke research, optical imaging of functional changes in the cerebral cortex and recovery utilizing well-established animal modeling approaches such as middle cerebral artery occlusion (MCAO) [28, 41, 78] or photothrombosis [37, 65, 66]. Typical cortical cranial window size varies from 2 mm up to 8 mm in diameter depending on the region of interest (ROI). Examples include synaptic and dendritic changes in retrosplenial cortex (posterior cortical area) with small-sized CW (~3 mm in diameter) by 2PE imaging [79]; OIS changes in small targeted region (visual cortex, ~4 mm) using intact skull cranial window model [80]; cerebral blood flow changes in somatosensory area (~6 mm in diameter) by LSCI and OISI [35]; large area (7 mm×8 mm) cortical neuronal connectivity analysis with VSDI [34]; and whole skull optical clearing window (SOWC) for microvessels and synaptic resolution [81].

Windows for deep brain region

Conventional transcranial windows only have a direct access to the cortical areas leaving subcortical or deep brain regions hardly accessible with optical techniques. As an example, the hippocampus, a prominent target for early detection of Alzheimer's disease (AD), is located below the cortex in rodents. Special type of cranial windows were constructed utilizing a gradient-index (GRIN) lens [68] or a triangular prism [73] for longitudinal observation of the deep brain target such as the hippocampus or cerebellum. These examples show that for longitudinal *in vivo* imaging, cranial window preparation is a valuable technique for observing disease progression *in situ*.

Spinal cord chamber window (SCCW)

The spinal cord chamber window is another cranial and spinal window type to achieve long-term imaging of the spinal cord. Spinal cord serves as an intermediate channel for nerve signals between the cerebrum and the peripheral nerves. While the cerebrum has been a predominant research subject in neuroscience, research on the spinal cord, which bridges the brain and peripheral nerve, has become increasingly important with the increased focus on peripheral nerve disorders. Previously, imaging for lumbar [37] or thoracic [36] has been majorly shown, which is straightforward to access and significant in size even for a small mouse, but lately, cervical imaging has also been tried [38]. SCCW was used for long-term monitoring of brain cancer metastases through the blood-brain barrier (BBB) [37, 38] or the response of astrocytes and microglias to ischemic brain injury [36]. Spinal cord with SCCW was observed after spinal injury through microglia inflammation and heterogenous dieback of axon stumps [69, 70]. Studies on neurorehabilitation or functional recovery of the spinal cord injury model are expected to be active when the SCCW model is combined with neuromodulation approaches.

Types of cranial and spinal windows

The early cranial and spinal window for brain imaging in small animals was a one-off procedure that involved drilling the skull down till the brain was exposed. For long-term *in vivo* imaging, the next generation of cranial and spinal windows covered the brain parenchyma with glass coverslip over the open-skull or thinned skull. However, these window types require further modification, including the retractable type or flexible polymer-based windows, which have been adopted in conjunction with other neuroscience techniques such as brain stimulation or electrophysiological recording [30, 39, 40, 77, 80, 82-84]. With advances in MEMS supported by nanotechnology, flexible transparent microelectrode will allow a range of previously unfeasible experiments due to the physical barrier from glass windows. Examples include functional brain mapping in response to optogenetic or ultrasound brain stimulation with freely moving mice during behavior tests. Fig. 2 shows schematic diagrams for typical types of cranial windows. We illustrate the examples of cranial and spinal windows for optical neuroimaging *in vivo* in Table 1, comparing animal subjects, cranial and spinal window types, optical imaging methods, and test apparatus from references.

Open-skull preparation

The open-skull preparation was used to monitor the blood-oxygen-level-dependent (BOLD) or optical intrinsic signal from the sensory, barrel, or visual cortex evoked by specific stimulation for observation under anesthesia [33]. Although this preparation was straightforward and yielded clear optical resolution, it came with the risk of inflammation during and after the imaging. This preparation method was the early form for optically observing the brain, and it has been used on small animals like mice and rats as well as medium and large mammals like cats and monkeys [85, 86]. A more recent study demonstrates a modified open-skull preparation method for ultrasound and photoacoustic mesoscopic imaging, covering the exposed cerebral cortex by suturing the scalp [43]. In the recent study, the exposed brain was coated with the hydrophilized 130 nm–thick-nanosheet of the polyethylene-oxide-coated CYTOP (PEO-CYTOP), which enabled *in vivo* deep

https://doi.org/10.5607/en22015

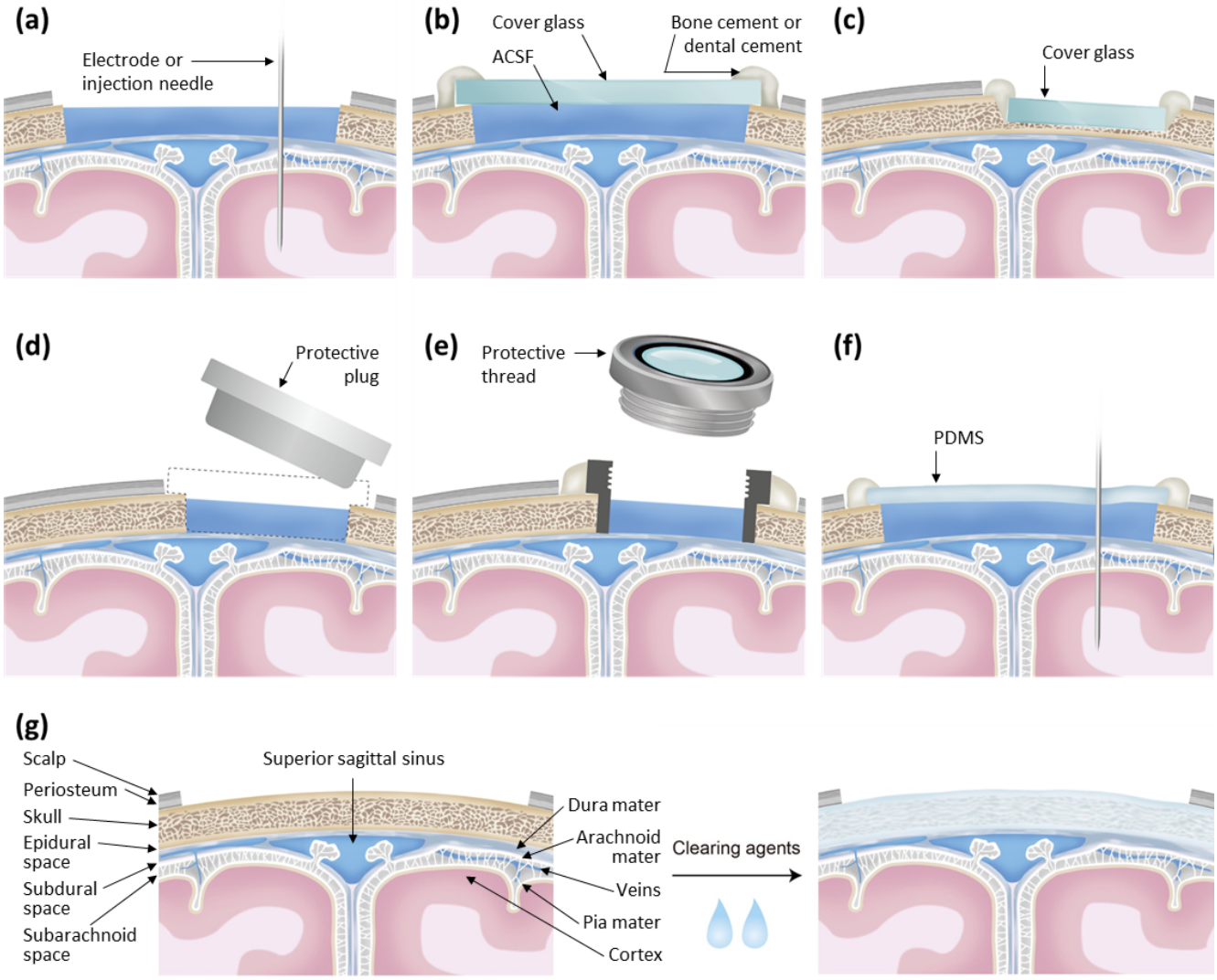

Fig. 2. Types of the cranial and spinal window. (a) Open-skull cranial window, (b) sealed cranial window, (c) thinned-skull cranial window, (d) a plug type open-close window, (e) threaded retractable cranial window, (f) flexible PDMS-based accessible window, and (g) skull optical clearing window (SOCW). The cranial window thins down or removes a part of the skull and then takes proper steps for safe and long-term observation. The window structure, material, and size can be varied by the research objectives. Open skull preparation, sealed cranial window, and thinned-skull cranial window are the traditional forms of the cranial window. In contrast, variously modified forms have been developed, such as open-close, retractable and accessible windows, to combine with other neuroscience methodologies.

brain imaging in a wide FOV, resulting in good adhesiveness to the brain surface. It also aided in the long-term control of surface bleeding and inflammation [87, 88].

Sealed cranial windows (closed cranial window)

Meanwhile, the sealed cranial window with glass coverslip [16, 19, 89], agarose [90], or silicon oil [65, 90] has been applied to protect the covering of the exposed cortical surface. Compared to the previously mentioned open skull preparation, this procedure allowed for mid or long-term observation [20, 91]. It has been used to observe the metastasis of brain tumors [92-96] and changes in brain tissue caused by a focal stroke [28, 41]. Anesthesia conditions, body temperature, and breathing should be managed for long-term and longitudinal observation. Furthermore, the choice of the glass window depends on the animal size and the duration of the experiment. Sometimes the dura mater is removed for securing image resolution with potential impairment of microenvironment physiology. This sealed window method allows mid to long-term observation, although the imaging duration can be limited due to the skull regrowth phenomenon. In addition, the imaging quality may be compromised by astrocytic gliosis and the undesired inflammatory response with microglial activation [97].

Table 1. The cranial and spinal windows for optical neuroimaging *in vivo*

Subject	Animal	Mouse	Mouse	Mouse	Mouse	Mouse	Mouse	Mouse	Mouse
	Species	Male B6CBAF1 or female Thy1.2YFP-H	YFP-H, CX3CR1-GFP, CX3CR1-GFP x YFP-H, Emx-1-cre, GFAP-GFP	Thy1-YFP-H and GFP-M (neuron) Balb/c and C57BL/6 wild-type (glioma)	Female transgenic C57BL/6 expressing GCaMP6s/f and GFP-m	C57BL/6 male	C57BL/6, Ai95(RCL-GCaMP6f)-D, NG2-CreERT2, Thy1-GCaMP6f	Sox9 cKO: Sox9fl/fl; CAG-CreER; Aldh1L1-EGFP Control: Sox9fl/fl; Aldh1L1-EGFP	G7NG817, Thy1-EYFP-H
	Anesthetization	Awake	Anesthetized with isoflurane	Anesthetized with isoflurane	Awake	Anesthetized with isoflurane	Awake	Anesthetized with isoflurane	Awake or anesthetized with isoflurane
	Region of interest	Primary sensory cortical areas (S1HL[a])	Spinal cord: vertebrae (T10-T12[b])	CA1[c] hippocampal pyramidal neuron dendrites, cerebral microvasculature	Sensory and motor cortex	Primary sensory cortical areas (S1FL[d], S1HL)	Olfactory bulb	Olfactory bulb	Primary visual cortex (V1[e])
Window	Window type	Open-close window (plug)	Open-close window (plug)	Modified sealed cranial window	Thinned-skull or intact skull window	Sealed cranial window	Sealed cranial window	Thinned-skull window	PEO-CYTOP[f] nanosheet
	Window size	~4 mm in diameter	5 mm in diameter	0.84 mm in diameter	~ 9×9 mm	6 mm in diameter		2~3 mm in diameter	> 8 mm in diameter
	Window material	Glass coverslip	Metal bars, glass coverslip	Glass capillary, glass coverslip, stainless steel screws	Glass coverslip, steel head bar	Anodized titanium	A titanium head-bar, glass coverslip	Glass coverslip	PEO-CYTOP nanosheet
	Bonding material	N/A	Dental acrylic and cyanoacrylate	Dental acrylic, UV curing epoxy	Mixture of metabond and dental cement	Dental cement	Photopolymerizable dental cement	N/A	UV curable dental acrylic
Optical imaging	Imaging technique	2PE-CaSDI	2PEF	1PEF and 2PEF	OISI	OISI, LSCI	2PE-CaSDI	2PE-CaSDI	2PEF, 2PE-CaSDI
	Measuring frequency (temporal resolution)	(256 msec/ frame)	N/A	100 Hz (up to 1.2 kHz)	30 Hz	10 Hz/5 Hz (200 msec/ 400 msec)	(50~150 msec/ frame)	10~35 Hz	1 Hz for EYFP, 30 Hz for GCaMP7, 3.8 Hz (CaSDI)
	Measuring time	4~5 min	N/A	Multiple sessions (30~60 min)	30 sec or 11.5 and 5 min	20 sec	N/A	10 sec/trial	N/A
	Objective lens	40X/0.8 NA[f]	20X/1.0 NA water-immersion, 40X/0.8 NA, water-immersion, 4X/0.28 NA	10X/0.25 NA, 20X/0.40 NA (1PEF) 10X/0.25 NA (2PEF)	Adjustable lens (f[g]=3.6 mm)	4X/0.10 NA	60X/1.10NA, 40X/0.8NA	20X/1.0 NA	16X/0.80 NA water-immersion (cross-sectional imaging), 25X/1.10 NA water-immersion (deep *in vivo* imaging), 2X/0.20NA (CaSDI)
Test & Apparatus	Animal test	Spherical treadmill running training	Open field and runway assays	N/A	Automated self-head-fixation and visual-evoked cortical imaging	Somatosensory-evoked functional imaging	Synaptic activity triggers odor-specific OPC[h] process	Three compartment place preference assay	CaSDI in vast FOV, deep and wide-field imaging
	Behavior test apparatus	Air-supported free-floating Styrofoam ball	Plexiglass enclosure to enter a dark goal box at the end of the runway	N/A	Fully automated and self-initiated head-fixation system for functional imaging, yellow light flash stimulator	Electrical sensory stimulator	Sensory stimulation, running wheel with head fixed	A testing chamber, video with a behavior tracking camera (for odor discrimination)	N/A
	Life supporting system	N/A	Rectal thermometer and feedback-controlled heating blanket at 37.5°C	Heating blanket	N/A	37°C heating pad	36.5~37°C heating pad, pneumogram transducer	Heating pad	Disposable heating pad
Ref.	Published year	2007	2012	2011	2016	2016	2018	2021	2020, 2021
	First author	Dombeck, D. A.	Farrar, M. J.	Barretto, R. P. J.	Murphy, T. H.	Cho, A.	Rungta, R. L.	Ung, K.	Takahashi, T.

The cranial and spinal window types were varied by the research objectives, animal condition and optical imaging methods.
[a]S1HL primary somatosensory hindlimb cortex; [b]T10-T12 tenth to twelfth thoracic vertebra; [c]CA1 the first region in the hippocampal circuit; [d]S1FL primary somatosensory forelimb cortex; [e]V1 primary visual cortex; [f]NA numerical aperture; [g]f focal length; [h]OPC oligodendrocyte precursor cell.

https://doi.org/10.5607/en22015

Open-close/retractable/accessible window

On the other hand, hybrid cranial windows have addressed the shortcomings of both open-skull preparation and sealed cranial windows while maximizing the benefits. The sliding-top cranial window has a chamber, thread, and slipover cap to obtain stable and simultaneous brain imaging and electrical recording. This method eliminated two significant problems that are cardiac and respiration-induced image artifacts and brain infection caused by contamination [98]. Similarly, retractable plugs on the glass coverslip were used to assess the recording electrode for the brain surface [30, 67, 84]. Meanwhile, a flexible and transparent polymer-based cranial window enabled the recording electrode or injection needle to penetrate the window surface. Other examples of hybrid windows are artificial dura [55] and accessible cranial windows [19]. Although the open-close, retractable, and accessible windows are relatively safe, there still exists a risk of infection and contamination by external assessment.

Thinned-skull preparation

The thinned-skull preparation, which involves grinding the skull until the skull becomes thin enough to be optically transparent, was invented to mitigate the shortcomings of the open-skull method, such as disrupting the local environment and potential contamination. By reporting the optical view while preventing direct exposure of the cortical surface through the skull thinning process, this technique also addresses the issues of the sealed cranial window. Although imaging resolution is limited due to the small residual skull layer and dura mater, image quality degradation caused by skull growth and gliosis can be minimized, allowing for more scientifically controlled observation [29, 78, 97, 99-101].

Skull optical clearing window (SOCW)

The optical tissue clearing window technique applies the optical clearing solution (SOCS) on the skull surface instead of the craniotomy [81, 102]. The SOCS included collagenase, EDTA disodium, and glycerol. The skull optical clearing window (SOCW) is easy to handle, and the SOCW technique is safe and reliable as no apparent inflammatory responses were reported associated with the SOCS. As a result, SOCW is well suited to studying microglia that are highly sensitive to the microenvironment. Although SOCS can make the skull almost entirely transparent, it works only for a short period. Thus, repeatedly SOCS may be necessary. Through the SOCW preparation, the minimum diameter of microvessels was measured as 14.4±0.8 μm closed to that of the exposed microvessels as 12.8±0.9 μm [102]. In addition, the imaging depth was achieved down to 250 μm below the pial surface [81]. Therefore, the SOCW could be an alternative approach for extensive thinning or removing the skull.

Material-based window classification

The previous classification was based on the different types of cranial and spinal windows; however, the window model can also be categorized based on the materials used. The original cranial window was prepared by placing a cover glass over the exposed brain surface. In contrast, the nanocrystalline material called yttria-stabilized zirconia (YSZ) was used to reinforce the glass's mechanical vulnerability. Compared to glass, YSZ has a higher hardness, and its biocompatibility is well established. The transparency is lower than that of glass when used for optical coherence tomography (OCT) imaging, but it ensures superior image quality compared to the native skull [103-107]. On the contrary, there are cases where transparent and flexible polydimethylsiloxane (PDMS) has been used to cover the cerebral cortex. Also, PDMS can be employed as the substrate of electrode fabrication. Electrode patterns were transcribed using silicon, graphite, graphene, or carbon nanotubes (CNTs) to electrically stimulate the cerebral cortex and optically record responses [39, 82, 83, 108, 109]. Furthermore, local field potential (LFP) recording was attempted with optical imaging with flexible and penetrable PDMS window [40, 77]. Meanwhile, a 35 μm collagen membrane sheet was used as an artificial dura substitute with high biocompatibility and semi-permeability to allow VSD dye to pass. Although this chemically and optically transparent collagen membrane made VSD staining easier, its utility for longitudinal investigation needs to be examined [110]. These examples highlight the proper choice of window materials based on the study purpose and observation method.

Various applications of the cranial and spinal window based on ROI, type, and material are illustrated. From the original single observation of a medium-large animal for an easy-to-access brain region, the cranial and spinal window has evolved for a mid and long-term observation of target CNS regions with small animal disease models. The practical issues will be addressed in the following section.

EXTENSIVE USE OF CRANIAL AND SPINAL WINDOW WITH OTHER APPARATUS

Combining with other neuroscience methodology

The cranial window preparation for the brain *in vivo* imaging has also been used to observe changes in the cerebral cortex combined with other methodologies. First of all, cranial windows have been used to see the response to brain stimulations such as optogenetic [6, 34, 111, 112], electrical [39], or ultrasound stimulation methods [113]. The window material is chosen according to

Table 2. The advanced cranial and spinal windows applying to optical neuroimaging combined with other neurological research methods

Subject	Animal	Mouse	Rat	Mouse	Mouse	Rat and mouse	Mouse
	Species	B6.Cg-Tg(Thy1-COP4/EYFP)18Gfng/J	Male Sprague Dawley rats	Thy1-GCaMP3, wild-type	VGAT-ChR2-EYFP BAC, Scnn1a-TG3-Cre x Ai32	C57BL6, Cx3Cr1G-FP+/− mice	Thy1-ChR2-YFP, GAD67-GFP10, wild-type ICR mice.
	Anesthetization	Anesthetized with isoflurane	Anesthetized with isoflurane	Awake	Anesthetized with isoflurane (OISI), awake (2PE-CaSDI)	Anesthetized with isoflurane	Anesthetized with isoflurane
	Region of interest	Primary sensory cortex (S1FL, S1HL), barrel cortex (S1BC[a]), visual cortex (V1), and auditory cortex (A1[b])	Somatosensory cortex	Somatosensory cortex	Barrel cortex (C2), somatosensory (S1), and frontal area (ALM[c])	Somatosensory cortex	Barrel cortex
Window	Window type	Sealed cranial window	Partial open skull window	Sealed cranial window	Open-close window (plug)	Accessible window	Sealed cranial window
	Window size	7 mm×8 mm bilateral, 7 mm×6 mm unilateral	5 mm in diameter	3~3.5 mm in diameter 8 mm round coverslip	3 mm in diameter	6 mm in diameter	~ 4×4 mm
	Window material	Glass coverslip	Glass coverslip	Glass coverslip	Glass coverslip	Glass coverslip, PDMS film	Glass coverslip, metal holding bar
	Bonding material	Mixture of dental cement and polyacrylic glue	UV curable dental acrylic	Mixture of dental cement and polyacrylic glue	Optical curable glue, dental acrylic	Cyanoacrylate glue and a dental resin	Dental acrylic
Optical imaging	Imaging technique	VSDI	Vascular fluorescence imaging	2PE-CaSDI, OISI	2PE-CaSDI, OISI	2PEF, OISI	2PEF, 2PE-CaSDI, OISI
	Measuring frequency (temporal resolution)	150 Hz (6.67 msec/frame)	N/A	10 Hz	7.8 Hz per plane (2PE-CaSDI)	10 Hz (OISI)	25~50 Hz (2PEF line scan), 10 Hz (CaSDI), 18 Hz (OISI)
	Measuring time	108 frames (~720 msec)	N/A	6 min	8 sec (2PE-CaSDI), 20 sec (OISI)	5 min (2PEF), 20 sec (OISI)	N/A
	Objective lens	5X/0.15 NA, 20X/0.50 NA	N/A	N/A	16x/0.8 NA	25X/0.95 NA or 10X/0.22 NA (2PEF)	4X/0.28 NA, 5X 0.16NA, 20X/0.5 NA
Test & Apparatus	Objectives	Comparison of sensory-evoked cortical maps with ChR2[d]-evoked cortical maps	N/A	Habituation-dishabituation olfactory test, smell recognition	Photoinhibition of barrel cortex during wall tracking	Electrical stimulation	Vascular and electrical responses to optogenetic photostimulation
	Combined methodology	Sensory stimulation, Optogenetic stimulation, electroencephalogram (EEG)	Micro-ECoG[e] devices (epidurally)	Patch-clamp recordings evoked cortical activity	Optogenetic stimulation, sensory stimulation (whisker), extracellular electrophysiology	Hindpaw electrical stimulation	LFP[f] measurements using the transparent graphene array
	Additional apparatus	Piezoelectric device for sensory stimulator	N/A	Air-lifted mobile homecage	Tactile virtual reality system for head-fixed mice running on a spherical treadmill, movable walls for whisker stimulation, laser photostimulation system	Inserting 30-gauge needle electrodes, connected to a pulse isolator and pulse stimulator	Stimulation device
	Life supporting system	37°C heating pad	Pulse oximeter	N/A	37°C heat blanket	36.5~37.5°C heating pad	N/A
Ref.	Published year	2012	2013	2014	2015	2016	2018
	First author	Lim, D. H.	Schendel, A. A.	Kislin, M.	Sofroniew, N.J	Heo, C.	Thunemann, M.

This table shows the multi-functional cranial and spinal windows or special designed cranial and spinal windows to combine neuroimaging and other neuroscience methodologies such as EEG, ECoG, patch clamp or Optogenetic stimulation, simultaneously.
[a]S1BC primary somatosensory; [a]S1BC barrel cortex; [b]A1 primary auditory cortex; [c]ALM anterior lateral motor cortex; [d]ChR2 channelrhodopsin-2; [e]ECoG electrocorticography; [f]LFP local field potential.

brain stimulation type, considering permeability and interference. Moreover, optical brain imaging was performed simultaneously with neuroelectrical recordings such as patch-clamp [40, 80, 84], electrocorticography (ECoG) [114], and electroencephalography (EEG) [33]. As the rodents' skull size ranges from mm to cm-scale, proper spatial arrangement is required [115, 116]. Microelectrodes have also been developed by microelectromechanical systems (MEMS) technology to record simultaneously optical and electrical neural activity [108, 114, 117]. On the other hand, chemicals such as a dye can facilitate structural observation or acquiring functional brain signals including blood flow responses following drug administration [67, 84]. Furthermore, multiple methods were combined for the observation of simultaneous electrical and optical signals from the brain [39, 40, 71, 84, 91]. Table 2 shows the advanced cranial and spinal windows to observe rodent brain combined with other neuroscience methodologies. The practical examples of cranial and spinal windows utilized for optical neuroimaging combined with other neuroscience methodologies are described in Fig. 3.

https://doi.org/10.5607/en22015

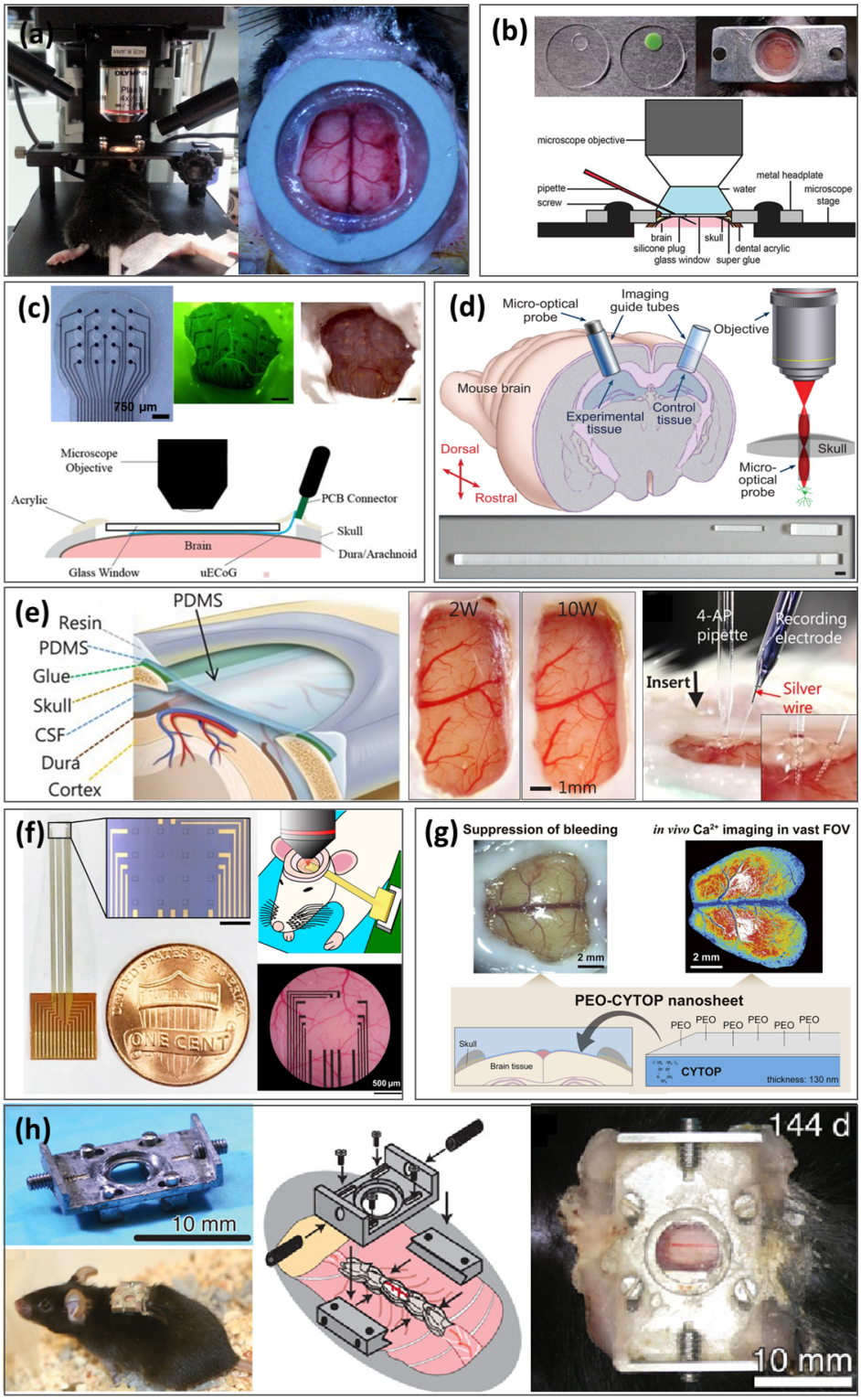

Fig. 3. Examples of cranial and spinal window; (a) a sealed cranial windows (closed cranial window) (an original image), (b) a plug type open-close/retractable/accessible window (Reproduced with permission, Copyright 2014, Frontiers [84]), (c) a window with implanted micro-ECoG multi-channel electrode array and 12 holes (Reproduced with permission, Copyright 2013, Elsevier [114]), (d) a cranial window utilizing a gradient-index (GRIN) lens and endoscopy targeting hippocampus (Reproduced with permission, Copyright 2011, Springer Nature [68]), (e) a flexible PDMS-based accessible window (Reproduced with permission, Copyright 2016, Springer Nature [40]), (f) transparent graphene microelectrode arrays (Reproduced with permission, Copyright 2018, Springer Nature [108]), (g) modified open skull window with PEO-CYTOP fluoropolymer nanosheets (Reproduced with permission, Copyright 2020, Elsevier [87]), and (h) spinal cord chamber window (SCCW) (Reproduced with permission, Copyright 2012, Springer Nature [21]).

Behavioral tests with awake animal models

Many brain imaging experiments through the cranial window model have been performed with animals under anesthesia. However, *in vivo* imaging with an awake animal undergoing a behavioral task is gaining popularity to avoid the anesthetic effect. Furthermore, freely behaving animals have been studied with EEG recording or equipped with a miniaturized microscope; however, these methods have limitations in single-cell level registration over large-area for brain connectivity. The optical window-based *in vivo* imaging system can be combined with a special apparatus during behavioral testing. For example, various treadmills have been used for studying exercise-induced behavioral recovery and neuroplasticity changes, such as straight treadmills [118-121] and ball-type treadmills [30, 73, 79, 122]. Other device types include a flat-floored air-lifted platform [123] and virtual reality (VR) environments [73, 118, 124], enabling the tracking of mouse locomotor activity while imaging. In addition, learning and memory function has been studied with spatial perception based on hippocampal place cell activity. Meanwhile, an automated home-cage mesoscopic functional imaging [125] showed visually-evoked cortical maps from multiple mice with a longitudinal study over three months.

The previously described apparatuses were not typical rodent behavioral tests such as elevated maze or conditioned cages have been used for functional recovery with well-defined rodent disease models and behavioral test paradigm. However, one limitation of such studies was the behavioral test and cellular recording were performed separately, and not integratable. Thus, optical neuroimaging techniques integrated with other modalities along with behavioral experiments, allows powerful integration of results and direct explanation the functional change and recovery mechanisms at the cellular resolution with a disease model. We are observing the expansion of optical neuroimaging apparatuses together with conventional behavioral assays with specific disease model, such as stroke [126] or Alzheimer's disease [127].

DISCUSSION

Upon construction of the cranial and spinal window, the cover material's optical, chemical, and physical characteristics must be considered in accordance with the study's purpose and objectives. In order to optimize the quality of target images, region of interest (ROI), field of view (FOV), and tissue depth should be specified, from which the optical imaging parameters and experimental setting can be selected. In addition to the camera sensor area, the number of pixels, and window glass material, including refractive index, and the working distance of the objective lens needs to be determined prior to the window-making procedure. Moreover, since it is applied to live animals, selecting the window's physical strength and an appropriate weight is also necessary for the long-term preservation of the window and subsequent observation. As much as physical and chemical properties, the factors concerning animal species and conditions should also be considered. In other words, materials and shapes of the cranial window need to be selected based on the species, age, size, weight, life expectancy, the type of animal disease model, location of ROI, and size of FOV.

As for species-dependent differences, the rat and mouse have a considerable difference in life expectancy and physical strength. Therefore, such phenotypic differences should be taken into account, as the window strength and durability for rats and the whole window weight for mice may become significant factors. For example, a flexible polymer-based window may require additional protection depending on the observation period and animal size. Although highly effective, typical optical imaging methods using the cranial and spinal window exhibit both benefits and limitations. While the cranial and spinal window enables efficient 2D wide-field imaging, information collected from optical neuroimaging often suffers from the constraint of superficial information. For studies of 3D functional neurodynamics, simultaneous acquisition of neuroelectric signals using electrophysiology in the targeted brain areas at variable depths can be adopted [39, 42, 63, 108, 117].

Combined electrophysiological recording and optical imaging have been attempted to reveal synaptic responses and cortical activity with high spatio-temporal resolution in large populations of cortical neurons. This multimodal approach enables electro-optic mapping of cellular neuronal activity and ultimately correlates circuit-level behavior and the connectivity among different brain regions [40, 73, 79, 117]. Of cautioning note, the insertion of electrodes would induce unavoidable damage to the tissue, and the imaging FOV would also be restricted by the electrode. Single electrode insertion to the exposed brain could be sufficient in some cases; [63, 67, 89] however, specialized design and devices (e.g., micro electric mechanical system: MEMS) and/or implementation of multi-channel recording setup may be necessary for effective assessment of the 3D neural structures [39, 42, 108, 117].

When performing imaging using a cranial and spinal window with a behaving animal, spatial arrangements of the microscope stage are crucial considering FOV, the working distance of the objective lens, anesthesia setting, and proper monitoring of the animal under experiment. In conjunction with a recording or behavioral test, sequential procedures with involved devices should also be considered in multimodal imaging. Progressive habituation protocols are necessary for awaked rodent imaging with

https://doi.org/10.5607/en22015

head-fixed circumstances, to adapt the animal to the restrained condition [31, 123, 125]. Developing a behavioral test scenario is necessary while considering spatial allowance, temporal resolution limitation, and the maximum measurement duration per single imaging run. A virtual reality (VR) environment can be implemented for a freely-moving-like environment to extend to the *in vivo* optical imaging further using the cranial and spinal window.

Optical *in vivo* imaging using cranial and spinal windows can be compared to imaging with miniaturized microscopes (miniscopes). In general, using the cranial and spinal window provides more expandability to combine with other techniques and a larger optical FOV [128, 129]. Furthermore, multimodal imaging is easier for simultaneous acquisition of various data (neuronal activity, cerebral hemodynamics, structural imaging). On the other hand, miniscopes have evolved to integrate electrophysiology and calcium imaging in free-moving animals. Also, the miniscope approach is suitable for entirely free-moving or social interaction tests. Thus, the proper choice of approach depends on these considerations.

CONCLUSION AND FUTURE DIRECTIONS

Over the past decade, traditional cranial and spinal window-based optical *in vivo* imaging technology has slowly paved the way for high-resolution neuroimaging of living animals. Advances in optics, MEMS technology, and biocompatible materials allow versatile cranial and spinal window technology, which can be a paradigm change in neuroscience. This Review introduced various cranial and spinal window types used in the optical neuroimaging field with rodent window models for anesthetized and awake animals. The combination of window-based optical imaging with other imaging modalities such as ultrasound and MRI can provide further depth and dynamics to the study of the nervous system, which can be furthered with electrophysiology techniques.

The evolution of cranial and spinal windows has several important implications for future neuroscience practices. The future cranial and spinal window will find applications in functional brain mapping and reveal mechanisms of brain dysfunction at the cellular resolution with various disease animal models. For example, one could envisage using the cranial and spinal window with a behaving animal for longitudinal investigation on brain connectivity during optogenetic stimulation, neural plasticity changes, or testing new drug candidates related to various neurological diseases such as Alzheimer's disease, Parkinson's disease, stroke, epilepsy, and chronic pain. With ongoing progression in cranial and spinal window preparation, we expect transformable, multi-functional, or flexible cranial and spinal window to become commonplace in neuroscience laboratories alongside advances in neuroimaging modalities.

ACKNOWLEDGEMENTS

The work was supported by The GIST Research Institute (GRI) research collaboration grant funded by GIST in 2022 and the 2022 Joint Research Project of Institutes of Science and Technology, a grant from the National Research Foundation of Korea (N.R.F.) funded by the Korean government (MEST) (NRF-2019R1A2C2086003), and the Korea Medical Device Development Fund grant funded by the Korea government, the Ministry of Science and ICT, the Ministry of Trade, Industry and Energy, the Ministry of Health & Welfare, the Ministry of Food and Drug Safety (Project Number: 1711138096, KMDF_PR_ 220200901_0076), and the Brain Pool program funded by the Ministry of Science and ICT through the NRF of Korea (2021H1D3A2A01099707).

REFERENCES

1. Kerr JN, Denk W (2008) Imaging *in vivo*: watching the brain in action. Nat Rev Neurosci 9:195-205.
2. Kobat D, Durst ME, Nishimura N, Wong AW, Schaffer CB, Xu C (2009) Deep tissue multiphoton microscopy using longer wavelength excitation. Opt Express 17:13354-13364.
3. Safi AM, Chung E (2016) Biomedical *in vivo* optical imaging for disease espying and diagnosis. In: Biomedical engineering: frontier research and converging technologies (Jo H, Jun HW, Shin J, Lee SH, eds), pp 329-355. Springer, Cham.
4. Chung E, Yeon C, Jain RK, Fukumura D (2014) Uncovering tumor biology by intravital microscopy. Compr Biomed Phys 4:153-164.
5. Boyden ES, Zhang F, Bamberg E, Nagel G, Deisseroth K (2005) Millisecond-timescale, genetically targeted optical control of neural activity. Nat Neurosci 8:1263-1268.
6. Ayling OG, Harrison TC, Boyd JD, Goroshkov A, Murphy TH (2009) Automated light-based mapping of motor cortex by photoactivation of channelrhodopsin-2 transgenic mice. Nat Methods 6:219-224.
7. Kherlopian AR, Song T, Duan Q, Neimark MA, Po MJ, Gohagan JK, Laine AF (2008) A review of imaging techniques for systems biology. BMC Syst Biol 2:74.
8. Snell RS (2010) Clinical neuroanatomy. 7th ed. Lippincott Williams & Wilkins, Baltimore, MD.
9. Carter R, Aldridge S, Page M, Parker S (2014) The human brain book. 2nd ed. DK Publishing, London.
10. Zeman W (2016) Carigie's neuroanatomy of the rat. Elsevier, New York, NY.

11. Carter R, Parker S (2014) The brain book. Dorling Kindersley Ltd, London.
12. Maikos JT, Elias RA, Shreiber DI (2008) Mechanical properties of dura mater from the rat brain and spinal cord. J Neurotrauma 25:38-51.
13. Hillman EM (2007) Optical brain imaging *in vivo*: techniques and applications from animal to man. J Biomed Opt 12:051402.
14. Balas C (2009) Review of biomedical optical imaging—a powerful, non-invasive, non-ionizing technology for improving *in vivo* diagnosis. Meas Sci Technol 20:104020.
15. Isshiki M, Okabe S (2014) Evaluation of cranial window types for *in vivo* two-photon imaging of brain microstructures. Microscopy (Oxf) 63:53-63.
16. Levasseur JE, Wei EP, Raper AJ, Kontos AA, Patterson JL (1975) Detailed description of a cranial window technique for acute and chronic experiments. Stroke 6:308-317.
17. Holtmaat A, Bonhoeffer T, Chow DK, Chuckowree J, De Paola V, Hofer SB, Hübener M, Keck T, Knott G, Lee WC, Mostany R, Mrsic-Flogel TD, Nedivi E, Portera-Cailliau C, Svoboda K, Trachtenberg JT, Wilbrecht L (2009) Long-term, high-resolution imaging in the mouse neocortex through a chronic cranial window. Nat Protoc 4:1128-1144.
18. Forbes HS (1928) The cerebral circulation: I. Observation and measurement of pial vessels. Arch NeurPsych 19:751-761.
19. Dóra E (1984) A simple cranial window technique for optical monitoring of cerebrocortical microcirculation and NAD/NADH redox state. Effect of mitochondrial electron transport inhibitors and anoxic anoxia. J Neurochem 42:101-108.
20. Morii S, Ngai AC, Winn HR (1986) Reactivity of rat pial arterioles and venules to adenosine and carbon dioxide: with detailed description of the closed cranial window technique in rats. J Cereb Blood Flow Metab 6:34-41.
21. Farrar MJ, Bernstein IM, Schlafer DH, Cleland TA, Fetcho JR, Schaffer CB (2012) Chronic *in vivo* imaging in the mouse spinal cord using an implanted chamber. Nat Methods 9:297-302.
22. Figley SA, Chen Y, Maeda A, Conroy L, McMullen JD, Silver JI, Stapleton S, Vitkin A, Lindsay P, Burrell K, Zadeh G, Fehlings MG, DaCosta RS (2013) A spinal cord window chamber model for *in vivo* longitudinal multimodal optical and acoustic imaging in a murine model. PLoS One 8:e58081.
23. Haghayegh Jahromi N, Tardent H, Enzmann G, Deutsch U, Kawakami N, Bittner S, Vestweber D, Zipp F, Stein JV, Engelhardt B (2017) A novel cervical spinal cord window preparation allows for two-photon imaging of t-cell interactions with the cervical spinal cord microvasculature during experimental autoimmune encephalomyelitis. Front Immunol 8:406.
24. Cramer SW, Carter RE, Aronson JD, Kodandaramaiah SB, Ebner TJ, Chen CC (2021) Through the looking glass: a review of cranial window technology for optical access to the brain. J Neurosci Methods 354:109100.
25. Wang Y, Xi L (2021) Chronic cranial window for photoacoustic imaging: a mini review. Vis Comput Ind Biomed Art 4:15.
26. Koletar MM, Dorr A, Brown ME, McLaurin J, Stefanovic B (2019) Refinement of a chronic cranial window implant in the rat for longitudinal *in vivo* two-photon fluorescence microscopy of neurovascular function. Sci Rep 9:5499.
27. Kim J, Bixel MG (2020) Intravital multiphoton imaging of the bone and bone marrow environment. Cytometry A 97:496-503.
28. Sigler A, Murphy TH (2010) *In vivo* 2-photon imaging of fine structure in the rodent brain: before, during, and after stroke. Stroke 41(10 Suppl):S117-S123.
29. Marker DF, Tremblay ME, Lu SM, Majewska AK, Gelbard HA (2010) A thin-skull window technique for chronic two-photon *in vivo* imaging of murine microglia in models of neuroinflammation. J Vis Exp 43:2059.
30. Dombeck DA, Khabbaz AN, Collman F, Adelman TL, Tank DW (2007) Imaging large-scale neural activity with cellular resolution in awake, mobile mice. Neuron 56:43-57.
31. van Beest EH, Mukherjee S, Kirchberger L, Schnabel UH, van der Togt C, Teeuwen RRM, Barsegyan A, Meyer AF, Poort J, Roelfsema PR, Self MW (2021) Mouse visual cortex contains a region of enhanced spatial resolution. Nat Commun 12:4029.
32. Xie Y, Chan AW, McGirr A, Xue S, Xiao D, Zeng H, Murphy TH (2016) Resolution of high-frequency mesoscale intracortical maps using the genetically encoded glutamate sensor iGluSnFR. J Neurosci 36:1261-1272.
33. Devonshire IM, Dommett EJ, Grandy TH, Halliday AC, Greenfield SA (2010) Environmental enrichment differentially modifies specific components of sensory-evoked activity in rat barrel cortex as revealed by simultaneous electrophysiological recordings and optical imaging *in vivo*. Neuroscience 170:662-669.
34. Lim DH, Mohajerani MH, Ledue J, Boyd J, Chen S, Murphy TH (2012) *In vivo* large-scale cortical mapping using channelrhodopsin-2 stimulation in transgenic mice reveals asymmetric and reciprocal relationships between cortical areas. Front Neural Circuits 6:11.
35. Cho A, Yeon C, Kim D, Chung E (2016) Laser speckle contrast imaging for measuring cerebral blood flow changes caused by electrical sensory stimulation. J Opt Soc Korea 20:88-93.

36. Guilbert J, Desjardins M (2022) Movement correction method for laser speckle contrast imaging of cerebral blood flow in cranial windows in rodents. J Biophotonics 15:e202100218.
37. Qureshi MM, Liu Y, Mac KD, Kim M, Safi AM, Chung E (2021) Quantitative blood flow estimation *in vivo* by optical speckle image velocimetry. Optica 8:1092-1101.
38. Qureshi MM, Brake J, Jeon HJ, Ruan H, Liu Y, Safi AM, Eom TJ, Yang C, Chung E (2017) *In vivo* study of optical speckle decorrelation time across depths in the mouse brain. Biomed Opt Express 8:4855-4864.
39. Heo C, Lee SY, Jo A, Jung S, Suh M, Lee YH (2013) Flexible, transparent, and noncytotoxic graphene electric field stimulator for effective cerebral blood volume enhancement. ACS Nano 7:4869-4878.
40. Heo C, Park H, Kim YT, Baeg E, Kim YH, Kim SG, Suh M (2016) A soft, transparent, freely accessible cranial window for chronic imaging and electrophysiology. Sci Rep 6:27818.
41. Mohammadzadeh L, Latifi H, Khaksar S, Feiz MS, Motamedi F, Asadollahi A, Ezzatpour M (2020) Measuring the frequency-specific functional connectivity using wavelet coherence analysis in stroke rats based on intrinsic signals. Sci Rep 10:9429.
42. Shabir O, Pendry B, Lee L, Eyre B, Sharp PS, Rebollar MA, Drew D, Howarth C, Heath PR, Wharton SB, Francis SE, Berwick J (2022) Assessment of neurovascular coupling and cortical spreading depression in mixed mouse models of atherosclerosis and Alzheimer's disease. Elife 11:e68242.
43. Wang X, Luo Y, Chen Y, Chen C, Yin L, Yu T, He W, Ma C (2021) A skull-removed chronic cranial window for ultrasound and photoacoustic imaging of the rodent brain. Front Neurosci 15:673740.
44. Provansal M, Labernède G, Joffrois C, Rizkallah A, Goulet R, Valet M, Deschamps W, Ferrari U, Chaffiol A, Dalkara D, Sahel JA, Tanter M, Picaud S, Gauvain G, Arcizet F (2021) Functional ultrasound imaging of the spreading activity following optogenetic stimulation of the rat visual cortex. Sci Rep 11:12603.
45. Carter M, Shieh J (2015) Guide to research techniques in neuroscience. 2nd ed. Academic Press, London.
46. Zong W, Wu R, Li M, Hu Y, Li Y, Li J, Rong H, Wu H, Xu Y, Lu Y, Jia H, Fan M, Zhou Z, Zhang Y, Wang A, Chen L, Cheng H (2017) Fast high-resolution miniature two-photon microscopy for brain imaging in freely behaving mice. Nat Methods 14:713-719.
47. Homma R, Baker BJ, Jin L, Garaschuk O, Konnerth A, Cohen LB, Bleau CX, Canepari M, Djurisic M, Zecevic D (2009) Wide-field and two-photon imaging of brain activity with voltage- and calcium-sensitive dyes. Methods Mol Biol 489:43-79.
48. Rubart M (2004) Two-photon microscopy of cells and tissue. Circ Res 95:1154-1166.
49. Horton NG, Wang K, Kobat D, Clark CG, Wise FW, Schaffer CB, Xu C (2013) *In vivo* three-photon microscopy of subcortical structures within an intact mouse brain. Nat Photonics 7:205-209.
50. White BR, Bauer AQ, Snyder AZ, Schlaggar BL, Lee JM, Culver JP (2011) Imaging of functional connectivity in the mouse brain. PLoS One 6:e16322.
51. Vanni MP, Chan AW, Balbi M, Silasi G, Murphy TH (2017) Mesoscale mapping of mouse cortex reveals frequency-dependent cycling between distinct macroscale functional modules. J Neurosci 37:7513-7533.
52. Guevara E, Sadekova N, Girouard H, Lesage F (2013) Optical imaging of resting-state functional connectivity in a novel arterial stiffness model. Biomed Opt Express 4:2332-2346.
53. Vincis R, Lagier S, Van De Ville D, Rodriguez I, Carleton A (2015) Sensory-evoked intrinsic imaging signals in the olfactory bulb are independent of neurovascular coupling. Cell Rep 12:313-325.
54. Devor A, Sakadžić S, Srinivasan VJ, Yaseen MA, Nizar K, Saisan PA, Tian P, Dale AM, Vinogradov SA, Franceschini MA, Boas DA (2012) Frontiers in optical imaging of cerebral blood flow and metabolism. J Cereb Blood Flow Metab 32:1259-1276.
55. Lu HD, Chen G, Cai J, Roe AW (2017) Intrinsic signal optical imaging of visual brain activity: tracking of fast cortical dynamics. Neuroimage 148:160-168.
56. Senarathna J, Rege A, Li N, Thakor NV (2013) Laser speckle contrast imaging: theory, instrumentation and applications. IEEE Rev Biomed Eng 6:99-110.
57. Briers D, Duncan DD, Hirst E, Kirkpatrick SJ, Larsson M, Steenbergen W, Stromberg T, Thompson OB (2013) Laser speckle contrast imaging: theoretical and practical limitations. J Biomed Opt 18:066018.
58. Wang HL, Chen JW, Yang SH, Lo YC, Pan HC, Liang YW, Wang CF, Yang Y, Kuo YT, Lin YC, Chou CY, Lin SH, Chen YY (2021) Multimodal optical imaging to investigate spatiotemporal changes in cerebrovascular function in AUDA treatment of acute ischemic stroke. Front Cell Neurosci 15:655305.
59. Grinvald A, Omer DB, Sharon D, Vanzetta I, Hildesheim R (2016) Voltage-sensitive dye imaging of neocortical activity. Cold Spring Harb Protoc 2016:pdb.top089367.
60. Chery R, L'Heureux B, Bendahmane M, Renaud R, Martin C,

Pain F, Gurden H (2011) Imaging odor-evoked activities in the mouse olfactory bulb using optical reflectance and autofluorescence signals. J Vis Exp 56:e3336.
61. Spors H, Grinvald A (2002) Spatio-temporal dynamics of odor representations in the mammalian olfactory bulb. Neuron 34:301-315.
62. Adam Y, Mizrahi A (2011) Long-term imaging reveals dynamic changes in the neuronal composition of the glomerular layer. J Neurosci 31:7967-7973.
63. Ung K, Huang TW, Lozzi B, Woo J, Hanson E, Pekarek B, Tepe B, Sardar D, Cheng YT, Liu G, Deneen B, Arenkiel BR (2021) Olfactory bulb astrocytes mediate sensory circuit processing through Sox9 in the mouse brain. Nat Commun 12:5230.
64. Rungta RL, Chaigneau E, Osmanski BF, Charpak S (2018) Vascular compartmentalization of functional hyperemia from the synapse to the pia. Neuron 99:362-375.e4.
65. Cianchetti FA, Kim DH, Dimiduk S, Nishimura N, Schaffer CB (2013) Stimulus-evoked calcium transients in somatosensory cortex are temporarily inhibited by a nearby microhemorrhage. PLoS One 8:e65663.
66. Dolezyczek H, Tamborski S, Majka P, Sampson D, Wojtkowski M, Wilczyński G, Szkulmowski M, Malinowska M (2020) *In vivo* brain imaging with multimodal optical coherence microscopy in a mouse model of thromboembolic photochemical stroke. Neurophotonics 7:015002.
67. Augustinaite S, Kuhn B (2021) Intrinsic optical signal imaging and targeted injections through a chronic cranial window of a head-fixed mouse. STAR Protoc 2:100779.
68. Barretto RP, Ko TH, Jung JC, Wang TJ, Capps G, Waters AC, Ziv Y, Attardo A, Recht L, Schnitzer MJ (2011) Time-lapse imaging of disease progression in deep brain areas using fluorescence microendoscopy. Nat Med 17:223-228.
69. Velasco MG, Levene MJ (2014) *In vivo* two-photon microscopy of the hippocampus using glass plugs. Biomed Opt Express 5:1700-1708.
70. Pilz GA, Carta S, Stäuble A, Ayaz A, Jessberger S, Helmchen F (2016) Functional imaging of dentate granule cells in the adult mouse hippocampus. J Neurosci 36:7407-7414.
71. Mathiesen C, Caesar K, Thomsen K, Hoogland TM, Witgen BM, Brazhe A, Lauritzen M (2011) Activity-dependent increases in local oxygen consumption correlate with postsynaptic currents in the mouse cerebellum *in vivo*. J Neurosci 31:18327-18337.
72. Askoxylakis V, Badeaux M, Roberge S, Batista A, Kirkpatrick N, Snuderl M, Amoozgar Z, Seano G, Ferraro GB, Chatterjee S, Xu L, Fukumura D, Duda DG, Jain RK (2017) A cerebellar window for intravital imaging of normal and disease states in mice. Nat Protoc 12:2251-2262.
73. Low RJ, Gu Y, Tank DW (2014) Cellular resolution optical access to brain regions in fissures: imaging medial prefrontal cortex and grid cells in entorhinal cortex. Proc Natl Acad Sci U S A 111:18739-18744.
74. Squire LR (2009) Encyclopedia of neuroscience. Vol. 2. Academic Press, Amsterdam.
75. Moon C, Yoo SJ, Han HS (2014) Smell. In: Encyclopedia of the neurological sciences (Aminoff MJ, Daroff RB, eds), 2nd ed, pp 216-220. Academic Press, San Diego, CA.
76. Aminoff MJ, Daroff RB (2014) Encyclopedia of the neurological sciences. 2nd ed. Academic Press, San Diego, CA.
77. Park H, You N, Lee J, Suh M (2019) Longitudinal study of hemodynamics and dendritic membrane potential changes in the mouse cortex following a soft cranial window installation. Neurophotonics 6:015006.
78. Li Y, Baran U, Wang RK (2014) Application of thinned-skull cranial window to mouse cerebral blood flow imaging using optical microangiography. PLoS One 9:e113658.
79. Voigts J, Harnett MT (2018) An animal-actuated rotational head-fixation system for 2-photon imaging during 2-d navigation. bioRxiv. doi: 10.1101/262543.
80. Nsiangani A, Del Rosario J, Yeh AC, Shin D, Wells S, Lev-Ari T, Williams B, Haider B (2022) Optimizing intact skull intrinsic signal imaging for subsequent targeted electrophysiology across mouse visual cortex. Sci Rep 12:2063.
81. Zhao YJ, Yu TT, Zhang C, Li Z, Luo QM, Xu TH, Zhu D (2018) Skull optical clearing window for *in vivo* imaging of the mouse cortex at synaptic resolution. Light Sci Appl 7:17153.
82. Li J, Xu J, Liu X, Zhang T, Lei S, Jiang L, Ou-Yang J, Yang X, Zhu B (2020) A novel CNTs array-PDMS composite with anisotropic thermal conductivity for optoacoustic transducer applications. Compos B Eng 196:108073.
83. Li H, Dong B, Zhang X, Shu X, Chen X, Hai R, Czaplewski DA, Zhang HF, Sun C (2019) Disposable ultrasound-sensing chronic cranial window by soft nanoimprinting lithography. Nat Commun 10:4277.
84. Roome CJ, Kuhn B (2014) Chronic cranial window with access port for repeated cellular manipulations, drug application, and electrophysiology. Front Cell Neurosci 8:379.
85. Navari RM, Wei EP, Kontos HA, Patterson JL Jr (1978) Comparison of the open skull and cranial window preparations in the study of the cerebral microcirculation. Microvasc Res 16:304-315.
86. Liu GB, Pettigrew JD (2003) Orientation mosaic in barn owl's visual Wulst revealed by optical imaging: comparison with cat and monkey striate and extra-striate areas. Brain Res 961:153-

158.
87. Takahashi T, Zhang H, Kawakami R, Yarinome K, Agetsuma M, Nabekura J, Otomo K, Okamura Y, Nemoto T (2020) PEO-CYTOP fluoropolymer nanosheets as a novel open-skull window for imaging of the living mouse brain. iScience 23:101579.
88. Takahashi T, Zhang H, Otomo K, Okamura Y, Nemoto T (2021) Protocol for constructing an extensive cranial window utilizing a PEO-CYTOP nanosheet for *in vivo* wide-field imaging of the mouse brain. STAR Protoc 2:100542.
89. Augustinaite S, Kuhn B (2020) Chronic cranial window for imaging cortical activity in head-fixed mice. STAR Protoc 1:100194.
90. Shih AY, Driscoll JD, Drew PJ, Nishimura N, Schaffer CB, Kleinfeld D (2012) Two-photon microscopy as a tool to study blood flow and neurovascular coupling in the rodent brain. J Cereb Blood Flow Metab 32:1277-1309.
91. Fujita H, Matsuura T, Yamada K, Inagaki N, Kanno I (2000) A sealed cranial window system for simultaneous recording of blood flow, and electrical and optical signals in the rat barrel cortex. J Neurosci Methods 99:71-78.
92. Jain RK, Safabakhsh N, Sckell A, Chen Y, Jiang P, Benjamin L, Yuan F, Keshet E (1998) Endothelial cell death, angiogenesis, and microvascular function after castration in an androgen-dependent tumor: role of vascular endothelial growth factor. Proc Natl Acad Sci U S A 95:10820-10825.
93. Hobbs SK, Monsky WL, Yuan F, Roberts WG, Griffith L, Torchilin VP, Jain RK (1998) Regulation of transport pathways in tumor vessels: role of tumor type and microenvironment. Proc Natl Acad Sci U S A 95:4607-4612.
94. Orringer DA, Chen T, Huang DL, Armstead WM, Hoff BA, Koo YE, Keep RF, Philbert MA, Kopelman R, Sagher O (2010) The brain tumor window model: a combined cranial window and implanted glioma model for evaluating intraoperative contrast agents. Neurosurgery 66:736-743.
95. Melder RJ, Salehi HA, Jain RK (1995) Interaction of activated natural killer cells with normal and tumor vessels in cranial windows in mice. Microvasc Res 50:35-44.
96. Kodack DP, Chung E, Yamashita H, Incio J, Duyverman AM, Song Y, Farrar CT, Huang Y, Ager E, Kamoun W, Goel S, Snuderl M, Lussiez A, Hiddingh L, Mahmood S, Tannous BA, Eichler AF, Fukumura D, Engelman JA, Jain RK (2012) Combined targeting of HER2 and VEGFR2 for effective treatment of HER2-amplified breast cancer brain metastases. Proc Natl Acad Sci U S A 109:E3119-E3127.
97. Dorand RD, Barkauskas DS, Evans TA, Petrosiute A, Huang AY (2014) Comparison of intravital thinned skull and cranial window approaches to study CNS immunobiology in the mouse cortex. Intravital 3:e29728.
98. Arieli A, Grinvald A (2002) Optical imaging combined with targeted electrical recordings, microstimulation, or tracer injections. J Neurosci Methods 116:15-28.
99. Yang G, Pan F, Parkhurst CN, Grutzendler J, Gan WB (2010) Thinned-skull cranial window technique for long-term imaging of the cortex in live mice. Nat Protoc 5:201-208.
100. Drew PJ, Shih AY, Driscoll JD, Knutsen PM, Blinder P, Davalos D, Akassoglou K, Tsai PS, Kleinfeld D (2010) Chronic optical access through a polished and reinforced thinned skull. Nat Methods 7:981-984.
101. Shih AY, Mateo C, Drew PJ, Tsai PS, Kleinfeld D (2012) A polished and reinforced thinned-skull window for long-term imaging of the mouse brain. J Vis Exp 61:3742.
102. Wang J, Zhang Y, Xu TH, Luo QM, Zhu D (2012) An innovative transparent cranial window based on skull optical clearing. Laser Phys Lett 9:469.
103. Damestani Y, Galan-Hoffman DE, Ortiz D, Cabrales P, Aguilar G (2016) Inflammatory response to implantation of transparent nanocrystalline yttria-stabilized zirconia using a dorsal window chamber model. Nanomedicine 12:1757-1763.
104. Damestani Y, Kodera Y, Garay J, Cabrales P, Aguilar G (2014) Biocompatibility and thermal profile of transparent nanocrystalline yttria-stabilized-zirconia calvarium prosthesis. Lasers Surg Med 46(S25): 35.
105. Damestani Y, Reynolds CL, Szu J, Hsu MS, Kodera Y, Binder DK, Park BH, Garay JE, Rao MP, Aguilar G (2013) Transparent nanocrystalline yttria-stabilized-zirconia calvarium prosthesis. Nanomedicine 9:1135-1138.
106. Halaney DL, Jonak CR, Liu J, Davoodzadeh N, Cano-Velázquez MS, Ehtiyatkar P, Park H, Binder DK, Aguilar G (2020) Chronic brain imaging across a transparent nanocrystalline yttria-stabilized-zirconia cranial implant. Front Bioeng Biotechnol 8:659.
107. Choi WJ (2019) Optical coherence tomography angiography in preclinical neuroimaging. Biomed Eng Lett 9:311-325.
108. Thunemann M, Lu Y, Liu X, KılıçK, Desjardins M, Vandenberghe M, Sadegh S, Saisan PA, Cheng Q, Weldy KL, Lyu H, Djurovic S, Andreassen OA, Dale AM, Devor A, Kuzum D (2018) Deep 2-photon imaging and artifact-free optogenetics through transparent graphene microelectrode arrays. Nat Commun 9:2035.
109. Kuzum D, Takano H, Shim E, Reed JC, Juul H, Richardson AG, de Vries J, Bink H, Dichter MA, Lucas TH, Coulter DA, Cubukcu E, Litt B (2014) Transparent and flexible low noise

graphene electrodes for simultaneous electrophysiology and neuroimaging. Nat Commun 5:5259.
110. Kunori N, Takashima I (2019) An implantable cranial window using a collagen membrane for chronic voltage-sensitive dye imaging. Micromachines (Basel) 10:789.
111. Ruiz O, Lustig BR, Nassi JJ, Cetin A, Reynolds JH, Albright TD, Callaway EM, Stoner GR, Roe AW (2013) Optogenetics through windows on the brain in the nonhuman primate. J Neurophysiol 110:1455-1467.
112. Harrison TC, Ayling OG, Murphy TH (2012) Distinct cortical circuit mechanisms for complex forelimb movement and motor map topography. Neuron 74:397-409.
113. Kim E, Anguluan E, Kim JG (2017) Monitoring cerebral hemodynamic change during transcranial ultrasound stimulation using optical intrinsic signal imaging. Sci Rep 7:13148.
114. Schendel AA, Thongpang S, Brodnick SK, Richner TJ, Lindevig BD, Krugner-Higby L, Williams JC (2013) A cranial window imaging method for monitoring vascular growth around chronically implanted micro-ECoG devices. J Neurosci Methods 218:121-130.
115. Kawakami M, Yamamura K (2008) Cranial bone morphometric study among mouse strains. BMC Evol Biol 8:73.
116. Yang P, Wang Z, Zhang Z, Liu D, Manolios EN, Chen C, Yan X, Zuo W, Chen N (2018) The extended application of The Rat Brain in Stereotaxic Coordinates in rats of various body weight. J Neurosci Methods 307:60-69.
117. Yin R, Noble BC, He F, Zolotavin P, Rathore H, Jin Y, Sevilla N, Xie C, Luan L (2022) Chronic co-implantation of ultraflexible neural electrodes and a cranial window. Neurophotonics 9:032204.
118. Giovannucci A, Pnevmatikakis EA, Deverett B, Pereira T, Fondriest J, Brady MJ, Wang SS, Abbas W, Parés P, Masip D (2018) Automated gesture tracking in head-fixed mice. J Neurosci Methods 300:184-195.
119. Heiney SA, Wohl MP, Chettih SN, Ruffolo LI, Medina JF (2014) Cerebellar-dependent expression of motor learning during eyeblink conditioning in head-fixed mice. J Neurosci 34:14845-14853.
120. Wienisch M, Blauvelt DG, Sato TF, Murthy VN (2011) Two-photon imaging of neural activity in awake, head-restrained mice. In: Neuronal network analysis (Fellin T, Halassa M, eds), pp 45-60. Humana Press, New York, NY.
121. Villette V, Levesque M, Miled A, Gosselin B, Topolnik L (2017) Simple platform for chronic imaging of hippocampal activity during spontaneous behaviour in an awake mouse. Sci Rep 7:43388.
122. Tran CH, Gordon GR (2015) Acute two-photon imaging of the neurovascular unit in the cortex of active mice. Front Cell Neurosci 9:11.
123. Kislin M, Mugantseva E, Molotkov D, Kulesskaya N, Khirug S, Kirilkin I, Pryazhnikov E, Kolikova J, Toptunov D, Yuryev M, Giniatullin R, Voikar V, Rivera C, Rauvala H, Khiroug L (2014) Flat-floored air-lifted platform: a new method for combining behavior with microscopy or electrophysiology on awake freely moving rodents. J Vis Exp 88:e51869.
124. Sofroniew NJ, Vlasov YA, Hires SA, Freeman J, Svoboda K (2015) Neural coding in barrel cortex during whisker-guided locomotion. Elife 4:e12559.
125. Murphy TH, Boyd JD, Bolaños F, Vanni MP, Silasi G, Haupt D, LeDue JM (2016) High-throughput automated home-cage mesoscopic functional imaging of mouse cortex. Nat Commun 7:11611.
126. Ruan J, Yao Y (2020) Behavioral tests in rodent models of stroke. Brain Hemorrhages 1:171-184.
127. Pentkowski NS, Rogge-Obando KK, Donaldson TN, Bouquin SJ, Clark BJ (2021) Anxiety and Alzheimer's disease: behavioral analysis and neural basis in rodent models of Alzheimer's-related neuropathology. Neurosci Biobehav Rev 127:647-658.
128. Wu X, Yang X, Song L, Wang Y, Li Y, Liu Y, Yang X, Wang Y, Pei W, Li W (2021) A modified miniscope system for simultaneous electrophysiology and calcium imaging *in vivo*. Front Integr Neurosci 15:682019.
129. Stamatakis AM, Resendez SL, Chen KS, Favero M, Liang-Guallpa J, Nassi JJ, Neufeld SQ, Visscher K, Ghosh KK (2021) Miniature microscopes for manipulating and recording *in vivo* brain activity. Microscopy (Oxf) 70:399-414.

https://doi.org/10.5607/en22015